Adaptive Gramian-Angular-Field Segmentation Integration Based Generative Adversarial Network (AGSI-GAN) for Eye Diagram Estimation of High Bandwidth Memory (HBM) Interposer

Junghyun Lee, Seonguk Choi, Keeyoung Son, Joonsang Park, Hyunwoo Kim, Keunwoo Kim, Taein Shin,
Boogyo Sim, Jonghyun Hong, Jiwon Yoon, Juneyoung Kim and Joungho Kim
School of Electrical Engineering, Korea Advanced Institute of Science and Technology (KAIST)
Daejeon, Republic of Korea
E-mail: junghyunlee@kaist.ac.kr

***Abstract*— In this paper, we propose an adaptive Gramian-Angular-Field segmentation integration (AGSI) based generative adversarial networks (GANs) for eye diagram estimation, which is a novel approach in high bandwidth memory (HBM) interposer design. The proposed AGSI framework effectively integrated relevant signal integrity (SI) components, namely single bit response (SBR) and far-end crosstalk (FEXT). AGSI allows for a customized and accurate representation of various design scenarios. By employing GAN-based estimator with AGSI as input data, the model significantly improved the time efficiency and accuracy of eye diagram estimation. This novel approach has potential applications in other domains, including signal integrity/power integrity (SI/PI) co-simulation, and is expected to enhance the design process in terms of time cost for HBM interposers and beyond.**

***Index Terms*—Adaptive Gramian-Angular-Field segmentation integration, eye diagram estimation, generative adversarial networks, high bandwidth memory**

I. Introduction

The growing demand for fast and powerful computing devices has led to the development of high bandwidth memory (HBM). HBM interposer design has become increasingly important due to the dense and compact channel routing resulting from the large number of input/outputs (I/Os) and data rate, which cause signal degradation [1]. Signal integrity (SI) challenges, such as channel loss, crosstalk, and inter-symbol interference (ISI), arise in HBM interposer, emphasizing the importance of maintaining signal quality despite design constraints. Therefore, designing a high-speed memory channel in the HBM interposer requires a comprehensive analysis of SI, including eye diagram analysis.

Since the process of eye diagram simulation is time-consuming, eye diagram estimation methods play a crucial role in reducing the time cost of the design process. Conventionally, peak distortion analysis (PDA) based method has been used to obtain the worst eye contour [2]. Nowadays, machine-learning based methods have emerged as a promising approach to further improve the time efficiency of the estimation [3]. However, these methods have faced limitations in generating complete eye diagrams. While it is possible to analyze performance by estimating key parameters of eye diagrams, understanding the specific SI element that require the improvement is not feasible. To address this issue, a generative adversarial networks (GANs) based eye diagram estimation has emerged as a promising alternative [4]. GANs, as generative models, can create complete eye diagrams, distinguishing them from conventional eye diagram estimation methodologies.

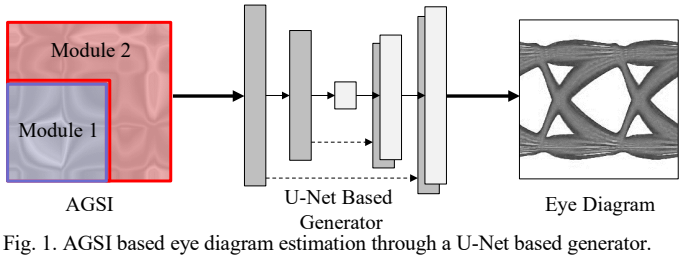

Fig. 1. AGSI based eye diagram estimation through a U-Net based generator.

The previous work employs the Gramian Angular Sum Field (GASF) as an input condition for GAN to capture ISI by transforming time-series data into images [4]. This method, which utilizes GASF as a condition, facilitates the generation of relevant eye diagrams. GASF is widely employed in computer vision approaches for processing, analyzing, and classifying tasks. By examining the trigonometric sum between each point of time-series data, it becomes easier to discern the temporal correlation across various time intervals [5]. However, the key limitation is its inability to process multiple datasets concurrently, restricting its usage in scenarios requiring comprehensive time-series analysis.

Therefore, in this paper, we propose the GAN-based eye diagram estimation method with the adaptive Gramian-Angular-Field segmentation integration (AGSI) framework. Fig. 1 highlights the usage of the AGSI framework as input in the generator for eye diagram estimation, emphasizing its role in the process. By adaptively extracting critical engineering factors from input data, our approach facilitated the integration of diverse information types. We demonstrated that the implementation of the proposed method in the HBM interposer design can effectively handle signals with multiple features. This technique offered improvements in efficiency and had the potential to benefit various applications, addressing limitations in existing eye diagram estimators.

II. Proposal of the Adaptive Gramian-Angular-Field Segmentation Integration (AGSI) Framework

In this section, GAN-based eye diagram estimator model is proposed. The estimator model applied the proposed AGSI

979-8-3503-1798-5/23/$31.00 ©2023 IEEE

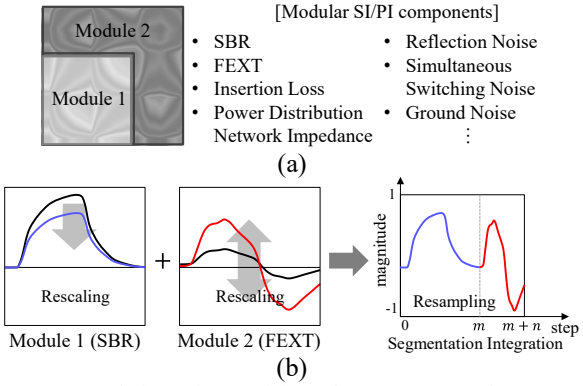

Fig. 2. (a) AGSI design using modular SI/PI components. (b) Segmentation integration of SBR and FEXT as modular SI components.

framework with segmentation integration of SI components as the estimator's input and performs an image-to-image translation using a conditional GAN (cGAN).

A. AGSI with modular SI/PI components

We propose the AGSI framework, an effective method for encoding multiple data into one image, which facilitates the integration of diverse information sources in a unified representation. This approach allowed for the application of GANs for accurate estimation in a wide array of domains and disciplines, by adaptively extracting essential engineering factors from the input data. In this paper, our AGSI framework, as shown in Fig. 2(a), was designed with the ability to accommodate both modular SI and power integrity (PI) components. These modular components can be freely chosen and configured, allowing for adjustments in the sequence and size according to the design importance of each component. We defined the AGSI by modifying GASF as:

$$AGSI = \begin{bmatrix} cos(\alpha_1 + \alpha_1) & \cdots & cos(\alpha_1 + \beta_n) \\ \vdots & \ddots & \vdots \\ cos(\alpha_m + \alpha_1) & \cdots & cos(\alpha_m + \beta_n) \\ cos(\beta_1 + \alpha_1) & \cdots & cos(\beta_1 + \beta_n) \\ \vdots & \ddots & \vdots \\ cos(\beta_n + \alpha_1) & \cdots & cos(\beta_n + \beta_n) \end{bmatrix} \quad (1)$$

Each α_i and β_j ($i = 1, 2, \ldots, m, j = 1, 2, \ldots, n$) represents the encoded values of the i-th step in module 1 data and the j-th step in module 2 data, respectively. The configuration of modules and sizes, limited by the processed image's pixel size, affects the AGSI given as a condition. As AGSI can encapsulate extensive data, this approach facilitates the generation of accurate and deterministic results.

In this article, HBM interposer design took into account the considerable variation depending on the channel loss and the significant impact of crosstalk between neighboring channels. Therefore, single bit response (SBR) and far-end crosstalk (FEXT) were selected as the target module 1 and 2, respectively. This was followed by a segmentation integration procedure as depicted in Fig. 2(b). In the process, feature scaling techniques were employed to normalize data, ensuring the uniform representation of various features. This allowed for an effective merging of the modules into a unified dataset by rescaling and resampling data.

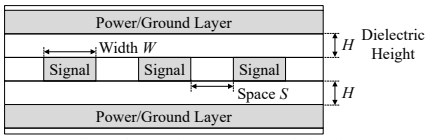

Fig. 3. HBM interposer stripline channel structure and the design parameters for the training dataset with variations in physical dimensions (*W, S, H*).

The proposed methodology employs the use of GASF in the process of representing difficult-to-understand signals with multiple features as images, rather than utilizing simply processed signal values through a network. This approach diverged from conventional applications of GASF, anticipating that signals from other domains, such as frequency-domain data, could also be utilized as feature-inclusive indicators through appropriate configuration.

B. Image-to-image translation with a conditional GAN

GANs consist of two primary components: a generator G, which aims to synthesize realistic data samples, and a discriminator D, which aims to distinguish between real and generated samples. GAN models learn to map from a random noise vector z to an output image y. However, cGANs extend this concept by learning mappings from both an input x and a random noise vector z to an output image y [6]. The cGAN's objective function can be denoted as:

$$\mathcal{L}_{cGAN}(G, D) = \mathbb{E}_{x,y}[\log D(x, y)] + \mathbb{E}_{x,z}[\log(1 - D(x, G(x, z)))] \quad (2)$$

This allows cGANs to generate images based on specific conditions or inputs, providing more control over the generated output compared to traditional GANs. In image-to-image translation using cGANs, employing a conditional image x as input, instead of random noise z, results in generating deterministic outcomes rather than stochastic ones [6]. We leveraged this aspect, and trained the GAN as an estimator for eye diagrams, where accuracy of the generated output is crucial. This approach efficiently utilized the deterministic nature of the output for practical applications in eye diagram estimation.

For the generator, a U-Net based generator could effectively utilize the features of AGSI to generate eye diagrams. Furthermore, to enhance the generated quality, PatchGAN discriminator was utilized to allow for the preservation of high-frequency information, while the addition of an L1 loss ensures the accurate capture of low-frequency details [6]. Consequently, this balanced distribution of roles enabled the design of a precise estimator to be implemented.

III. Data Generation and Preprocessing

For this work, we assumed the design space to be a stripline channel structure, as illustrated in Fig. 3. By modifying its physical dimensions, a dataset was generated for training purposes through ADS SPICE simulation tool. Assuming a progressive increase in the data rate for the next HBM2e, the data rate was set at 4.8 Gb/s. To ensure noticeable differences in the training dataset, the width, space, and dielectric height (*W, S, H*) of the channel, were set to have a step size of 0.2 μm and ranges of 1-3 μm, 1-3 μm, and 1-1.4 μm, respectively. The eye diagram simulation was set referring to JEDEC standard [7].

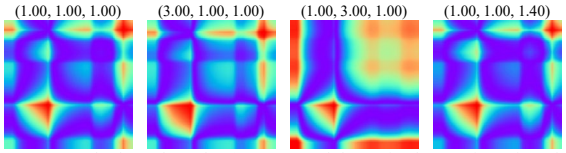

Fig. 4. AGSI results based on the (*W, S, H*) of the train dataset in units of μm.

In total, 363 eye diagrams and corresponding AGSI datasets were collected. The image size for both datasets is 256×256, with steps of AGSI module 1 and 2 configured as $m = 160$ and $n = 96$, respectively. The eye diagrams and AGSI training datasets were individually labeled and stored in separate hierarchical data format 5 (HDF5) files, streamlining data management and accessibility during network training.

The traditional GASF requires sufficient time-series data to encompass meaningful information. On the other hand, as demonstrated in Fig. 4, AGSI came up with the successful representation of channel characteristics using only the information of 2-bit signals corresponding to the 4 unit intervals (UI). The introduction of AGSI allowed for a mapping of SI-related impacts stemming from channel parameter changes (*W, S, H*) onto the RGB image space. This effectively showcases the capabilities and advantages of using AGSI to help GANs better understand channel behavior in various scenarios while relying on minimal input data.

IV. Verification of the Proposed AGSI-GAN based Eye Diagram Estimator for Design of HBM Interposer

After completion of 100 training epochs for each model, Table I presents the relative error between the ground truth and various eye diagram metrics for the following cases: applying GASF to SBR, applying GASF to pseudo-random bit sequence (PRBS) signals, and using AGSI as an input. When using only SBR as input, the network struggled to accurately interpret channel characteristics, which results in generated images that lack precision. PRBS allowed observing responses to various random bit patterns, providing more comprehensive information. However, PRBS also exhibited random errors exceeding 1% in eye height and width and fails to estimate overshoot.

In contrast, incorporating AGSI enabled the generated images to accurately reflect various eye diagram metrics, while maintaining similar input data generation time (t_{input}) as others. When utilizing the GPU resource GeForce RTX 3090, the inference time takes around 6.8 μs per sample, and the total elapsed time to perform channel simulation and obtain waveforms such as SBR & FEXT, as well as create AGSI, is less than 15 s. This breakthrough significantly reduced eye diagram simulation times, which typically range from several minutes to tens of minutes. Fig. 5(a) compares the generator's loss over

TABLE I
Comparison of Computational Time and Relative Error of Estimated Eye Diagram Metrics

Method	t_{input}	Eye height (error)	Eye width (error)	Overshoot (error)
GASF (SBR)	11.8 s	7.1 %	3.6 %	17.4 %
GASF (PRBS)	13.8 s	1.3 %	1.8 %	15.1 %
AGSI (SBR & FEXT)	13.9 s	0.4 %	0.4 %	3.3 %

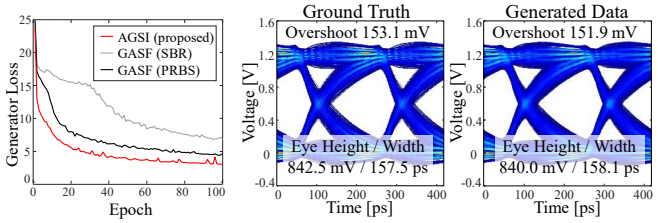

(a) (b)

Fig. 5. (a) Generator's loss over epochs for cGANs using GASF and AGSI. (b) Ground-truth and generated result with (*W, S, H*) = (1.10, 1.10, 1.30) in μm.

epochs for cGANs using each input, with AGSI demonstrating faster convergence. This indicates that incorporating AGSI into the input data design enables the network to learn from a wide data distribution, even with substantial step size changes across diverse design parameters. Fig. 5(b) shows the generated eye diagram which accurately represents all key parameters, with minimal blur and using previously unseen design parameters.

V. Conclusion

In conclusion, we demonstrated how SI/PI engineers can implement AGSI-GAN to develop more accurate and efficient estimators based on specific application requirements. The proposed AGSI-GAN based eye diagram estimator had significantly improved time efficiency maintaining high accuracy in HBM interposer design. The proposed AGSI estimation method can be extended to other target applications and performing SI/PI co-simulation with various components such as power induced noise. Additionally, the proposed method with reinforcement learning (RL) can be investigated for optimizing various design parameters.

Acknowledgment

We would like to acknowledge the technical support fro m ANSYS Korea. This research was supported by National R&D Program through the National Research Foundation of Korea (NRF) funded by Ministry of Science and ICT (NRF-2022M3I7A4072293). This work was supported by Samsung Electronics Co., Ltd (IO201207-07813-01, MEM230315_0004)

References

[1] S. Choi et al, "Sequential policy network-based optimal passive equalizer design for an arbitrary channel of high bandwidth memory using advantage actor critic.," in 2021 IEEE 30th Conference on Electrical Performance of Electronic Packaging and Systems (EPEPS), 2021, pp. 1-3.

[2] B. K. Casper, M. Haycock, and R. Mooney, "An accurate and efficient analysis method for multi-Gbps chip-to-chip signaling," in Proc. IEEE Symp. VLSI Circuits, pp. 54-57, Jun. 2002.

[3] D. Lho et al., "Eye-width and eye-height estimation method based on artificial neural network (ANN) for USB 3.0.", in 2018 IEEE 27th Conference on Electrical Performance of Electronic Packaging and Systems (EPEPS), 2018, pp. 209-211.

[4] P. Kashyap et al, "High speed receiver modeling using generative adversarial networks.", in 2021 IEEE 30th Conference on Electrical Performance of Electronic Packaging and Systems (EPEPS), 2021, pp. 1-3.

[5] Z. Wang and T. Oates, "Imaging time-series to improve classification and imputation," in International Joint Conference on Artificial Intelligence (IJCAI), 2015, pp. 3939–3945.

[6] P. Isola, J. Zhu, T. Zhou, and A. A. Efros, "Image-to-image translation with conditional adversarial networks," in IEEE Conference on Computer Vision and Pattern Recognition (CVPR), 2017, pp. 5967–5976.

[7] Standard, JEDEC, High Bandwidth Memory DRAM (HBM1, HBM2), JESD235D, 2021